JOURNAL OF THERMOPHYSICS AND HEAT TRANSFER
Vol. 7, No. 2, April–June 1993

Laminar Mixed Convection Flow in a Vertical Tube

A. Moutsoglou* and Y. D. Kwon†
South Dakota State University, Brookings, South Dakota 57007

A computational study is conducted to quantify the buoyancy effects on laminar forced flow of air in a heated/cooled vertical tube. Buoyancy assisting and buoyancy opposing flow cases are considered for heating/cooling rates that provide either uniform wall temperature or uniform heat flux conditions. The nature of the observed effects of various heating/cooling rates and configurations on the velocity and temperature development, as well as on flow reversal, is explained. Critical buoyancy parameters that signal the onset of flow reversal, as well as axial locations where flow reversal first occurs, are determined in the study. The effects of the buoyancy parameter on friction factors, Nusselt numbers, and flow and thermal entry lengths are documented.

Nomenclature

D = pipe diameter, m
f = local friction factor, $8\tau_w/\rho_\infty \bar{u}^2$
$\bar{f}$ = average friction factor, $8\bar{\tau}_w/\rho_\infty \bar{u}^2 = \int_0^x f\, dx/x$
Gr = Grashof number, $g\beta|T_w - T_\infty|R^3/\nu^2$ for UWT, or modified Grashof number, $g\beta|q_w|R^4/k\nu^2$ for UHF
g = gravitational acceleration, m/s^2
k = thermal conductivity, W/m-K
Nu_b = local bulk Nusselt number, $q_w D/k(T_w - T_b)$
$\overline{Nu}_b$ = average bulk Nusselt number, $Q_w D/2\pi Rxk(\bar{T}_w - \bar{T}_b)$
Nu_∞ = local ambient Nusselt number, $q_w D/k(T_w - T_\infty)$
$\overline{Nu}_\infty$ = average ambient Nusselt number, $Q_w D/2\pi Rxk(\bar{T}_w - T_\infty)$
$\bar{P}$, $\hat{P}$ = dimensionless mean pressure and dimensionless pressure variation from the mean
Pr = Prandtl number, ν/α
$\bar{p}$, $\hat{p}$ = mean and pressure variation from the mean, Pa
q_w = local wall heat flux to fluid, W/m^2
R = pipe radius, m
Re_D = Reynolds number, $\bar{u}D/\nu$
T = temperature, K
T_∞ = ambient temperature, K
T_b, $\bar{T}_b$ = local and average bulk temperatures, K
T_w, $\bar{T}_w$ = local and average wall temperatures, K
UHF = uniform heat flux
U, V = dimensionless axial and radial velocity components
UWT = uniform wall temperature
$\bar{u}$ = mean velocity, m/s
u, v = axial and radial velocity components, m/s
X = dimensionless axial coordinate, $4x/DRe_D$
x, r = axial and radial coordinates, m
α = thermal diffusivity, m^2/s
β = coefficient of thermal expansion, K^{-1}
η = dimensionless radial coordinate, r/R
θ = dimensionless temperature, $\theta = (T - T_\infty)/(T_w - T_\infty)$ for UWT, or $\theta = k(T - T_\infty)/q_w R$ for UHF
ν = kinematic viscosity, m^2/s
ρ, ρ_∞ = local and ambient densities, kg/m^3
τ_w, $\bar{\tau}_w$ = local and average wall shear stresses, N/m^2
Ω = buoyancy force parameter, $\pm Gr/Re_D$

Received Aug. 17, 1991; revision received March 2, 1992; accepted for publication March 5, 1992.

*Professor, Mechanical Engineering Department.
†Graduate Student, Mechanical Engineering Department.

Introduction

COMBINED forced and free convection in a vertical tube is one of the most extensively investigated mixed convection problems because of its application in heat exchangers and nuclear technology. A summary highlighting only some of the published computational and experimental studies for laminar mixed convection in a vertical tube is given in Table 1.

Despite the vast number of investigations on the subject, there seems to be no detailed account of published data accurately quantifying the buoyancy effects on the laminar flow and heat transfer characteristics in a heated or cooled vertical tube.[20] Thus, even though the buoyancy effects on forced flow have been established a while ago, no single study seems to present comprehensive data that are readily accessible to the thermal design engineer for pressure drop and heat transfer calculations in a heated or cooled vertical tube. The contribution of the present laminar numerical data to the plethora of already published results may be summarized as follows:

1) The buoyancy effects on the flow and thermal entry lengths are illustrated. No such specific data have been published in the past.

2) The critical buoyancy parameters signaling the onset of flow reversal for both assisting and opposing flow conditions are determined. These are compared to available experimental and numerical predictions. Axial locations where the first flow reversal is encountered are documented.

3) Extensive data are compiled illustrating the buoyancy effects on local and average friction factors and Nusselt numbers. They include data for both assisting and opposing flow conditions in an isothermally or uniformly heated/cooled vertical tube.

Analysis

The applicability of the presented data is limited by the modeling assumptions. Thus, the equations solved pertain to the steady, laminar, axisymmetric flow of a constant property fluid with a Prandtl number of 0.7 (characteristic of air). The axial diffusion of stress and heat are omitted from the governing set of equations. The parabolicity of the equations is completed by decoupling the streamwise and transverse pressure gradients in the two momentum equations. Although these assumptions jeopardize the accuracy of the data at low Reynolds numbers, at the same time they eliminate the dependence of the results on the Reynolds number itself. In addition, viscous energy dissipation is assumed to be negligible and as such no Eckert number dependence is associated with

Table 1 Summary of published computational and experimental data on laminar mixed convection in a vertical tube

Computational	UWT	Assisting	Refs. 1, 2, 10, 12, 13, 14, 17, 18, 19
		Opposing	Refs. 12, 17, 18
	UHF	Assisting	Refs. 2, 3, 4, 5, 8, 10, 11, 12, 16, 17
		Opposing	Refs. 3, 5, 8, 12, 17
Experimental	UWT	Assisting	Refs. 5, 6, 7, 14, 15
		Opposing	Refs. 5, 7, 15
	UHF	Assisting	Refs. 7, 9, 12, 16
		Opposing	Ref. 7

the data. Beyond the Boussinesq approximation, the effects of temperature and pressure on density and viscosity of the fluid are also omitted in an effort to simplify the presentation of the data. As a result, the dimensionless data are functions of only the buoyancy parameter Ω (Grashof-to-Reynolds number ratio) and the fluid Prandtl number Pr. Finally, the entrance velocity of the fluid is chosen to be uniform. This is appropriate in instances when the heating/cooling of the fluid commences at the point where the fluid enters the tube.

The steady laminar flow assumption needs special attention as natural convection effects can cause transition to an unsteady flow at Reynolds numbers much lower than those usually associated with transition to turbulence for forced convection flow. It has been established experimentally[7,12,21] that transition to an unsteady flow for buoyancy assisting flow cases precipitates from the gradual growth of small disturbances that are in sinuous motion. This is very similar to wave instability (Tollmien-Schlichting waves) present in external boundary-layer flows. For buoyancy opposing flow situations, on the other hand, the flow instability has been found to be associated with separation at the wall. Transition to an unsteady flow for this case is sudden, and it is preceded by an asymmetry in the flowfield as shown in downflow experiments.[7,21] Thus, whereas for assisting flow it is quite possible to have unstable flows without observing transition, for opposing flows transition to an unsteady flow occurs shortly after an unstable flow is initiated.

From the above, one can thus conclude that for buoyancy opposing flow conditions the onset of flow reversal near the wall also signals transition to unsteady flow. However, when the buoyancy assists the flow, the first occurrence of small disturbances associated with the streamwise velocity profile developing points of inflection does not necessarily signify transition. As a result, flow reversal occurs at downstream streamwise locations from the point of onset of the disturbances. Although it is not necessary for assisting flows to have a reversal in order for the flow to become unstable, experiments of upflow of water in an isothermally heated tube report[5,7,22] that unsteady flow always occurred downstream of the flow reversal. It was also observed that the upstream region of the reversed flow appeared quite stable. Experimental transition data for water flowing upward in a uniformly heated tube are given by Scheely and Hanratty[21] and by Lawrence and Chato[12] who also present an approximate transition criterion.

Consequently, the range of applicability of the current computational data, as far as the steady laminar flow assumption is concerned, can be established for opposing flow as the region where no flow reversal is detected. No such claim can be made for the assisting flow case where transition is explicitly a function of the Reynolds number in addition to the buoyancy force parameter. However, even though one may need to resort to experimental transition data or wave instability analyses to assess the applicability of the current data for the buoyancy assisting flow case, published experimental data[5] report that flow reversal was observed upstream of transition to unsteady flow.

The fluid which enters the tube at the uniform ambient temperature T_∞ may be flowing either upward or downward while it is being heated or cooled. The surface of the tube is assumed to be maintained at either a uniform temperature T_w (UWT) or have a prescribed uniform heat flux q_w (UHF). For downward flow the origin of the coordinate system is at the top of the tube where the fluid enters.

The nondimensional parabolized axisymmetric Navier-Stokes and energy equations for steady laminar flow along with corresponding boundary conditions can be written as

$$\frac{\partial U}{\partial X} + \frac{1}{\eta}\frac{\partial}{\partial \eta}(\eta V) = 0 \tag{1}$$

$$U\frac{\partial U}{\partial X} + V\frac{\partial U}{\partial \eta} = -\frac{d\bar{P}}{dX} + \frac{1}{\eta}\frac{\partial}{\partial \eta}\left(\eta\frac{\partial U}{\partial \eta}\right) + 2\Omega\theta \tag{2}$$

$$U\frac{\partial V}{\partial X} + V\frac{\partial V}{\partial \eta} = -\frac{\partial \hat{P}}{\partial \eta} + \frac{1}{\eta}\frac{\partial}{\partial \eta}\left(\eta\frac{\partial V}{\partial \eta}\right) - \frac{V}{\eta^2} \tag{3}$$

$$U\frac{\partial \theta}{\partial X} + V\frac{\partial \theta}{\partial \eta} = \frac{1}{Pr}\frac{1}{\eta}\frac{\partial}{\partial \eta}\left(\eta\frac{\partial \theta}{\partial \eta}\right) \tag{4}$$

$$U = 1,\ V = 0,\ \theta = 0,\ \bar{P} = 0 \quad \text{at} \quad X = 0 \tag{5a}$$

$$\frac{\partial U}{\partial \eta} = 0,\ V = 0,\ \frac{\partial \theta}{\partial \eta} = 0, \quad \text{at} \quad \eta = 0 \tag{5b}$$

$$U = 0,\ V = 0,\ \theta = 1\ (\text{UWT}) \quad \text{or} \quad \frac{\partial \theta}{\partial \eta} = 1\ (\text{UHF})$$

$$\text{at} \quad \eta = 1 \tag{5c}$$

The transformed dimensionless parameters are defined from

$$X = \frac{4x}{DRe_D}, \quad \eta = \frac{r}{R}, \quad U = \frac{u}{\bar{u}}, \quad V = \frac{v\mathrm{Re}_D}{2\bar{u}}$$

$$\bar{P} = \frac{\bar{p} \pm \rho_\infty g x}{\rho_\infty \bar{u}^2}, \quad \hat{P} = \frac{Re_D^2 \hat{p}}{4\rho_\infty \bar{u}^2} \tag{6}$$

$$\theta = \frac{T - T_\infty}{T_w - T_\infty} \quad \text{for UWT}$$

$$\theta = \frac{k(T - T_\infty)}{q_w R} \quad \text{for UHF}$$

where $Re_D = \bar{u}D/\nu$ is the Reynolds number based on D, and the plus or minus sign in the definition of the mean pressure in Eq. (6) pertains, respectively, to upward or downward flow.

In the above equations Ω is a measure of the intensity of the buoyancy force defined as

$$\Omega = \pm\frac{Gr}{Re_D} \tag{7}$$

In Eq. (7) Gr has a dual interpretation depending on the surface heating condition

$$Gr = \frac{g\beta|T_w - T_\infty|R^3}{\nu^2} \quad \text{for UWT}$$

$$Gr = \frac{g\beta|q_w|R^4}{k\nu^2} \quad \text{for UHF} \tag{8}$$

The plus and minus signs in front of the buoyancy force parameter that appear in the streamwise momentum equation denote, respectively, buoyancy assisting and buoyancy opposing flows. The buoyancy assists the flow, $\Omega > 0$, when the pipe is being heated for upward flow or being cooled for downward flow. On the other hand, the buoyancy opposes the flow, $\Omega < 0$, when the pipe is being cooled for upward flow or heated for downward flow.

Computational Procedure

The system of Eqs. (1–5) was solved using the well-documented finite-difference scheme of Pantankar,[23] while adopting a control volume suggested by Patankar and Spalding[24] for the streamwise momentum and energy Eqs. (2) and (4). The radial momentum Eq. (3) was solved at each cross-stream plane using the Simpler algorithm.[23] A variable axial step size that ranged from $\Delta X = 3 \times 10^{-5}$ near the inlet to 10^{-3} at the exit was utilized in the computations. Forty-six grid points were chosen in the radial direction. The grid interspacing varied in the radial direction to effect denser clustering of the grid points near the tube wall. Results from a mesh with 23 radial grid points and half the number of axial steps produced local friction factors and Nusselt numbers that differed by less than 1% for $X > 9 \times 10^{-4}$ from those predicted by the adopted mesh.

Results

Physical Parameters

The local and average friction factors are defined, respectively, from

$$f = \frac{8\tau_w}{\rho_\infty \bar{u}^2}, \qquad \bar{f} = \frac{8\bar{\tau}_w}{\rho_\infty \bar{u}^2} = \frac{1}{x}\int_0^x f\,dx \tag{9}$$

Local Nusselt numbers based on the wall-to-ambient and wall-to-bulk temperature differences, respectively, are evaluated from

$$Nu_\infty = \frac{q_w}{(T_w - T_\infty)}\frac{D}{k}, \qquad Nu_b = \frac{q_w}{(T_w - T_b)}\frac{D}{k} \tag{10}$$

where T_b is the bulk temperature defined from

$$T_b = \frac{2}{R^2}\int_0^R \frac{u}{\bar{u}} Tr\,dr \tag{11}$$

Corresponding average Nusselt numbers are defined as

$$\overline{Nu}_\infty = \frac{Q_w}{2\pi Rx(\bar{T}_w - T_\infty)}\frac{D}{k}, \qquad \overline{Nu}_b = \frac{Q_w}{2\pi Rx(\bar{T}_w - \bar{T}_b)}\frac{D}{k} \tag{12}$$

In the above equations, Q_w is the total rate of heat transfer to or from the fluid

$$Q_w = 2\pi R\int_0^x q_w\,dx \tag{13}$$

$\bar{T}_w$ is the average tube surface temperature, and $\bar{T}_b$ is the mean bulk temperature defined from

$$\bar{T}_w = \frac{1}{x}\int_0^x T_w\,dx, \qquad \bar{T}_b = \frac{1}{x}\int_0^x T_b\,dx \tag{14}$$

The flow entry length x_{fd} is defined as the axial distance where the centerline velocity is within 1% of its fully developed value. Specifically

$x \to x_{fd}$ when

$$\begin{cases} u(r=0,x) \to 0.99u(r=0, x\to\infty) \begin{cases} \text{for UWT and } \Omega \geq 0 \\ \text{or} \\ \text{for UHF and } \Omega \leq 0 \end{cases} \\ u(r=0,x) \to 1.01u(r=0, x\to\infty) \begin{cases} \text{for UWT and } \Omega < 0 \\ \text{or} \\ \text{for UHF and } \Omega \geq 40 \end{cases} \end{cases} \tag{15}$$

The thermal entry length $x_{t,fd}$ is defined as the axial distance where the local bulk Nusselt number is within 1% of its fully developed value. Thus

$x \to x_{t,fd}$ when

$$\begin{cases} Nu_b(x) \to 1.01Nu_b(x\to\infty) \begin{cases} \text{for UWT and } \Omega \geq 0 \\ \text{or} \\ \text{for UHF and } \Omega \leq 0 \end{cases} \\ Nu_b(x) \to 0.99Nu_b(x\to\infty) \begin{cases} \text{for UWT and } \Omega \leq -3 \\ \text{or} \\ \text{for UHF and } \Omega \geq 40 \end{cases} \end{cases} \tag{16}$$

The effects of the buoyancy parameter on the friction factors, Nusselt numbers, and flow and thermal developing regions are illustrated for gases with a Prandtl number of 0.7, flowing either upward or downward in a heated or cooled vertical tube. It is reiterated that the present data are based on uniform inlet velocity and temperature profiles at $x = 0$ [Eq. (5a)]. The depicted trends are best described from the buoyancy effects on the velocity and temperature profiles for each heating/cooling configuration.

Isothermally Heated or Cooled Vertical Tube

When the buoyancy force is absent, the near-the-wall fluid is decelerated continuously due to the wall shear until the parabolic fully developed velocity profile is attained. This results in the monotonic exponential decrease of the friction factors (Fig. 1) and Nusselt numbers (Fig. 4) for $\Omega = 0$.

When the buoyancy force assists the flow ($\Omega > 0$) the deceleration of the near-the-wall fluid due to shear is resisted by the buoyancy assisting forces that tend to accelerate the fluid near the wall, resulting in friction factors that exceed those of pure forced convection (Fig. 1). At sufficiently large

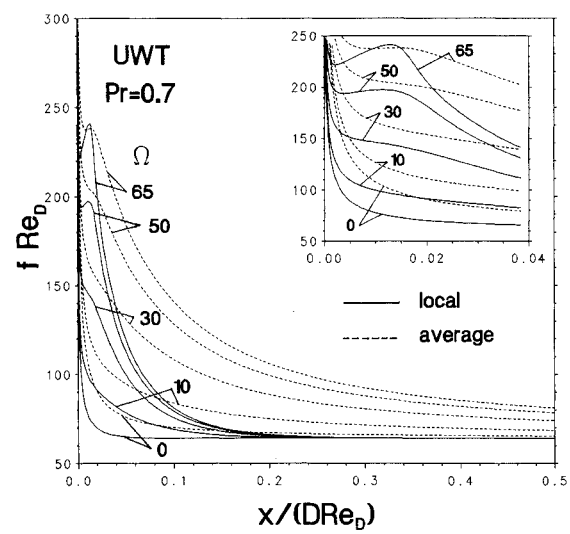

Fig. 1 Friction factors for buoyancy assisting flow in an isothermally heated or cooled vertical tube, $Pr = 0.7$.

buoyancy force parameters, $\Omega \geq 50$, the intensity of the buoyancy force overtakes the damping effect of the wall shear stress. This results in a net acceleration of the near-the-wall fluid and a subsequent increase in the local friction factor as indicated by the valleys for $\Omega = 50$ and 65 in Fig. 1 (inset). Farther downstream, the intensity of the buoyancy force diminishes as the fluid tends to the temperature of the wall. This results in a deceleration of the near-the-wall fluid accompanied by an acceleration of the center core fluid, resulting in the decrease of the local friction factors and the manifested peaks in Fig. 1. Finally, at sufficiently far distances from the inlet, the flow readjusts in the absence of any buoyancy force and attains the pure forced convection fully developed parabolic profile $u/\bar{u} = 2(1 - \eta^2)$, ensuing in the zero buoyancy fully developed friction factor of $f_{fd}Re_D = 64$. Furthermore, the initial deceleration of the near-the-wall fluid due to wall shear, followed by its acceleration due to assisting buoyancy forces and subsequent deceleration as the buoyancy force subsides, results in significantly longer flow entry lengths than pure forced convection case (see Fig. 3).

When the buoyancy force opposes the forced flow, the slowing down of the near-the-wall fluid due to wall shear is augmented further due to the opposing buoyancy force, resulting in friction factors that lie below those of pure forced convection (Fig. 2). Reduction of the near-the-wall velocities due to the opposing buoyancy forces is accompanied by an acceleration of the near-the-center core fluid, thus exceeding pure forced convection fully developed centerline velocities significantly. The diminishing of the intensity of the buoyancy force contributes to the occurrence of the valleys in the friction factors shown in Fig. 2. Eventually, as the fluid temperature

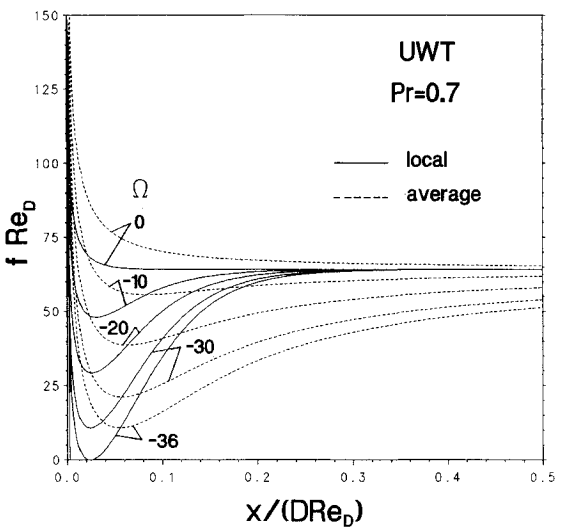

Fig. 2 Friction factors for buoyancy opposing flow in an isothermally heated or cooled vertical tube, $Pr = 0.7$.

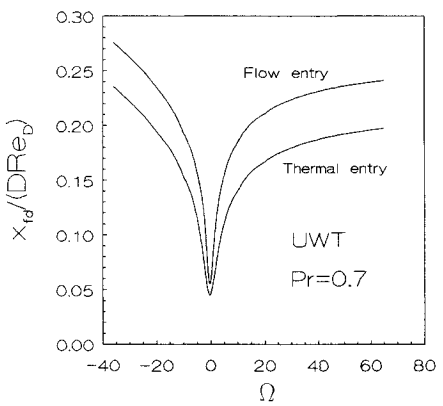

Fig. 3 Flow and thermal entry lengths in an isothermally heated or cooled vertical tube, $Pr = 0.7$.

nears the uniform wall temperature, the buoyancy force disappears and the fluid readjusts to attain the pure forced convection fully developed parabolic profile. Accordingly, the friction factors for opposing flow (Fig. 2) exhibit minima near the inlet of the pipe, while ultimately merging asymptotically to the zero buoyancy fully developed limit of $f_{fd}Re_D = 64$ at sufficiently large distances from the inlet. The augmentation of the deceleration of the near-the-wall fluid due to opposing buoyancy forces and the subsequent extinction of the buoyancy force results in significantly longer flow entry lengths (see Fig. 3).

When the buoyancy force assists the flow, the acceleration near the wall is accompanied by deceleration of the near-the-center fluid as dictated by the conservation of mass. Eventually, as the buoyancy force increases further, the centerline streamwise velocity reverses itself and the fluid near the centerline moves opposite to the entering flow in order to conserve mass. In these instances, the parabolicity of the equations is not satisfied and the present solution algorithm becomes invalid. In the present study for an isothermally heated/cooled tube with buoyancy assisting conditions, the onset of flow reversal occurred at a buoyancy parameter $\Omega_{crit} = 66$. This is smaller than $\Omega_{crit} = 89$ predicted for air by Zeldin and Schmidt[14] who used a coarser grid point mesh. Rosen and Hanratty[25] using an approximate analysis which employed a parabolic inlet velocity profile predicted flow inversion for $Pr = 0.73$ at $\Omega_{crit} = 73.5$. Scheely et al.[7] reported experimental transition data in terms of a Gr vs Re plot for upflow heating of water with constant wall temperature.

Flow reversal also occurs when the buoyancy force opposes the forced flow. This time, however, the reversal occurs near the wall due to the large buoyancy forces present near the surface where the fluid motion is relatively small. For the continuously heated/cooled isothermal tube the onset of flow reversal for buoyancy opposing case was determined at $\Omega_{crit} = -37$. Rosen and Hanratty[25] using an approximate method predicted Ω_{crit} to be -29. Flow visualization experiments using a dye reported by Scheely et al.[7] indicated the occurrence of an asymmetric region of reversed flow at $\Omega_{crit} = -37$ for constant temperature cooling of water in upflow. It is noted, however, that the experiments were conducted with an unheated starting length thus modeling a parabolic entrance velocity at the start of cooling. Transition data are also presented in the same study.[7]

Flow reversal, in the present study, for both buoyancy assisting and opposing flow cases occurred very close to the entrance of the pipe for the uniform wall temperature case, $[x/(DRe_D)]_{crit} = 0.016$ for $\Omega_{crit} = 66$ and $[x/(DRe_D)]_{crit} = 0.018$ for $\Omega_{crit} = -37$. It is interesting to note that the streamwise locations of flow reversal are way upstream of the fully developed conditions depicted in Fig. 3. This is because the largest temperature differences and buoyancy forces exist at the entrance of the pipe. As the buoyancy parameters increase beyond their corresponding critical values the onset of flow reversal moves upstream towards the inlet for both buoyancy assisting and buoyancy opposing cases. The approximate analysis of Rosen and Hanratty,[25] which employed a parabolic inlet velocity profile, predicted the axial locations where flow reversal first occurs to be $[x/(DRe_D)]_{crit} = 0.0189$ for $\Omega_{crit} = 73.5$ and $[x/(DRe_D)]_{crit} = 0.0516$ for $\Omega_{crit} = -37$. It is of interest to note the effects of the assumed inlet profile on flow reversal. If the heating/cooling of the pipe starts at a point beyond the flow entry length region, it is appropriate for the inlet velocity at the heated region to be that of a pure forced convection fully developed profile $u/\bar{u} = 2(1 - \eta^2)$. Due to the parabolic nature of the inlet velocity then, flow reversal will be delayed for buoyancy assisting flow while it will occur sooner for opposing flow cases. This is consistent with the numerical estimates for the buoyancy assisting flow of Zeldin and Schmidt,[14] where $\Omega_{crit} = 89$ for a uniform velocity profile at the entrance, whereas $\Omega_{crit} = 97$ for a fully developed parabolic profile at the inlet.

Consistent with the trends of the just discussed velocity profiles, when the buoyancy force assists the forced flow ($\Omega > 0$) the convective heat transfer rate from the heated ($T_w > T_\infty$) or to the cooled ($T_w < T_\infty$) wall is initially rejuvenated. This results in generally higher fluid temperatures for the heated wall, or lower fluid temperatures for the cooled wall than corresponding pure forced convection temperatures. Thus, this initial augmentation of the convective heat transfer rate is self-destructive as it diminishes the wall-to-fluid temperature difference that drives the heat transfer. Consequently, as the bulk Nusselt numbers are a measure of the ratio of the convective flux to the wall-to-bulk temperature difference, they exceed the zero buoyancy values as illustrated in Fig. 4. Eventually, at downstream locations where the buoyancy force disappears, the bulk Nusselt numbers attain asymptotically the zero buoyancy fully developed limit of $Nu_b = 3.66$. It is interesting to note that at the high buoyancy parameters, $\Omega \geq 50$, bulk Nusselt numbers exhibit kinks (Fig. 4) rather than the valleys and peaks shown in Fig. 1. This may be due to friction factors being directly affected by buoyancy forces, while Nusselt numbers are indirectly affected via the velocity profile.

Similarly, when the buoyancy force opposes the forced flow ($\Omega < 0$) the further deceleration of the near-the-wall fluid initially diminishes the heat transfer rate between the fluid and tube. This in turn augments the wall-to-fluid temperature difference. As a result, when the buoyancy opposes the flow, the bulk Nusselt numbers lie below those for zero buoyancy force and exhibit slight valleys as shown in Fig. 5. Again, at sufficiently far downstream locations, the buoyancy forces subside as the fluid attains the uniform wall temperature, and the local Nusselt numbers reach the zero buoyancy fully developed limit of $Nu_b = 3.66$.

Thermal entry lengths as defined from Eq. (16) are also plotted in Fig. 3. Consistent with the trends described for the flow entry length, the thermal entry lengths are also shown to increase with buoyancy force for both assisting and opposing flow cases. For a fluid with a Prandtl number of 0.7, the thermal entry lengths are slightly shorter than corresponding flow entry lengths. For the uniform wall temperature considered, the eventual disappearance of the buoyancy force destroys the coupling and the dependence of the velocity profile on the temperature distribution, thus resulting in the two separate (flow versus thermal) entry lengths shown in Fig. 3.

The Nusselt number based on the wall-to-bulk temperature difference is a measure of both the wall temperature gradient and the wall-to-bulk temperature difference. On the other hand, local Nusselt numbers based on wall-to-ambient temperature difference are directly a measure of the heat transfer rate from or to the wall.

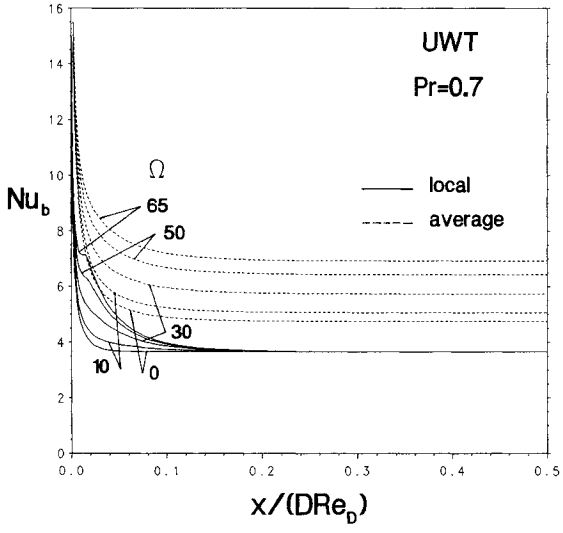

Fig. 4 Bulk Nusselt numbers for buoyancy assisting flow in an isothermally heated or cooled vertical tube, $Pr = 0.7$.

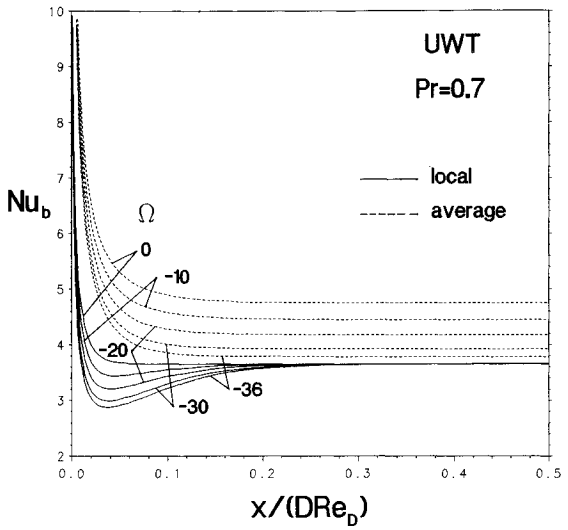

Fig. 5 Bulk Nusselt numbers for buoyancy opposing flow in an isothermally heated or cooled vertical tube, $Pr = 0.7$.

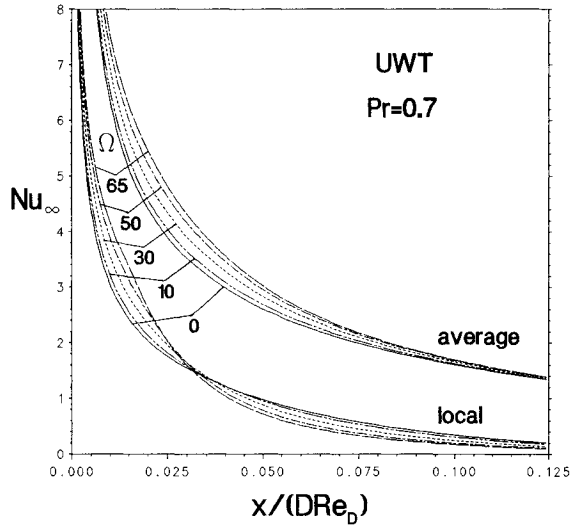

Fig. 6 Ambient Nusselt numbers for buoyancy assisting flow in an isothermally heated or cooled vertical tube, $Pr = 0.7$.

Such local and average ambient Nusselt numbers are plotted for an isothermally heated/cooled vertical tube in Figs. 6 and 7 for buoyancy assisting and opposing flows, respectively. As can be seen from Fig. 6, when the buoyancy assists the forced flow ($\Omega > 0$) higher Nusselt numbers are attained for the mixed convection flow near the inlet of the pipe due to increasing convective heat transfer rates that result from the accelerating flow near the wall. As noted earlier, the augmentation of the convective heat transfer rates near the entrance of the tube eventually diminishes the magnitude of the wall-to-fluid temperature difference. This reduction, therefore, causes the lowering of local mixed convection Nusselt numbers below corresponding local forced convection values. The crossover occurs at shorter distances from the inlet with increasing intensity of assisting buoyancy parameters (at $x/DRe_D) = 0.03125$ for $\Omega = 65$; at $x/(DRe_D) = 0.03975$ for $\Omega = 10$) as noted from Fig. 6. The exact opposite trend occurs for buoyancy opposing flow case as seen from Fig. 7. Thus, local convective heat transfer rates are initially below those for the forced convection case due to the buoyancy induced deceleration. However, at some point downstream, the ensuing larger wall-to-fluid temperature differences enhance the heat transfer mechanism, resulting in local Nusselt numbers that exceed their zero buoyancy values. The crossover of the

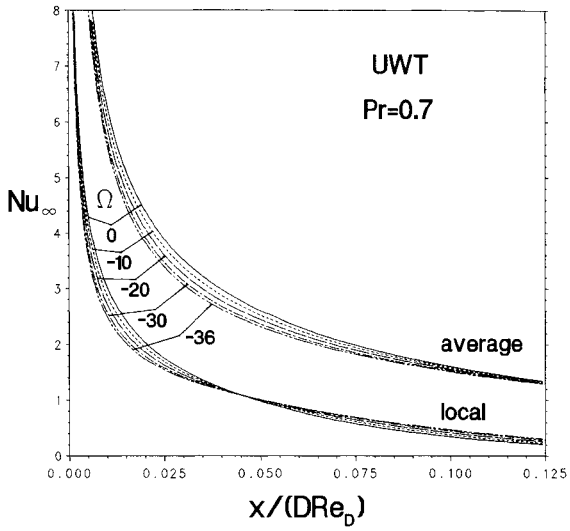

Fig. 7 Ambient Nusselt numbers for buoyancy opposing flow in an isothermally heated or cooled vertical tube, $Pr = 0.7$.

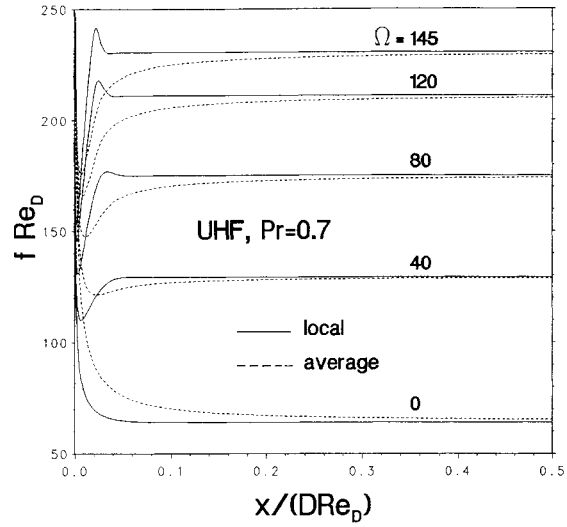

Fig. 8 Friction factors for buoyancy assisting flow in a uniformly heated or cooled vertical tube, $Pr = 0.7$.

local data with the zero buoyancy curve occurs around $x/(DRe_D) = 0.04545$.

From Eqs. (10) and (12), with the local heat flux and total heat transfer rates calculated from Figs. 6 and 7, one can determine corresponding local and mean bulk temperatures with the aid of Figs. 4 and 5.

Uniformly Heated or Cooled Vertical Tube

When the heating or cooling of the tube surface is prescribed by means of a uniform heat flux condition, heat is continuously pumped at the same rate to or from the fluid. Thus, even though the intensity of the buoyancy force decreases in the developing region, it attains a minimum and remains constant thereafter. Hence, in contrast to the UWT case where the dependence of the velocity on temperature ceases to exist beyond a region away from the inlet, for the uniform heat flux case the coupling of the momentum equation with the thermal field by way of the buoyancy force is present throughout the heated/cooled tube. One consequence of this coupling is the existence of a single flow/thermal developing region in contrast to the independent flow and thermal entry lengths present for the UWT case.

When the buoyancy force assists the flow ($\Omega > 0$) the shear related deceleration of the near-the-wall fluid is opposed by the buoyancy forces that tend to aid the motion of the fluid near the wall. This results in friction factors that exceed those of pure forced convection as shown in Fig. 8. Therefore, this buoyancy coupling induces the valleys in the local friction factors illustrated in Fig. 8. Away from the inlet, the intensity of the buoyancy force decreases resulting in the peaks shown in the same figure. Eventually, the decrease in the friction factors levels off as fully developed conditions are attained. The resultant fully developed velocity profiles, which are not parabolic anymore, exhibit maxima near the wall and minima at the center. Thus, for UHF as the ever-present buoyancy forces assist the flow, the thermal communication between the wall and the fluid is enhanced which results in shorter entry lengths. This is illustrated in Fig. 10 where the common flow/thermal entry length is plotted as a function of the buoyancy parameter.

When the buoyancy force opposes the forced flow ($\Omega < 0$), the shear related deceleration of the near-the-wall fluid is further augmented by the opposing buoyancy forces. This results in friction factors that lie below corresponding zero buoyancy values as shown in Fig. 9, and monotonically decrease to their fully developed values. The resultant fully developed velocity profiles exhibit maxima at the centerline that exceed the zero buoyancy parabolic value $u|_{r=0} = 2\bar{u}$. Since the negative buoyancy forces hinder the thermal communication between the wall and the fluid, longer entry lengths are experienced with increasing magnitude of the negative buoyancy forces, as illustrated in Fig. 10. Fully developed friction factors for both buoyancy assisting and buoyancy opposing flow cases are presented in Fig. 11.

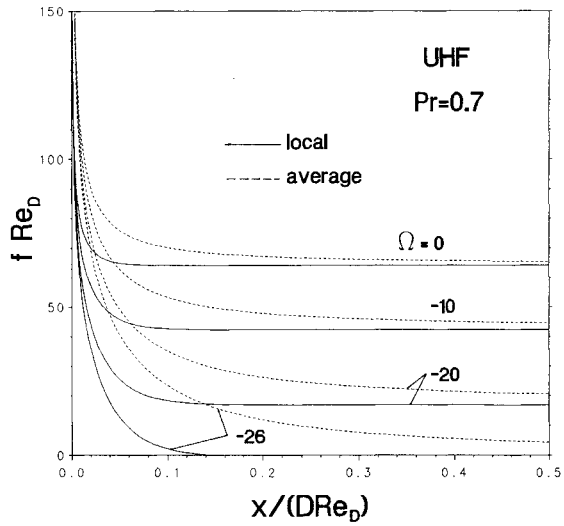

Fig. 9 Friction factors for buoyancy opposing flow in a uniformly heated or cooled vertical tube, $Pr = 0.7$.

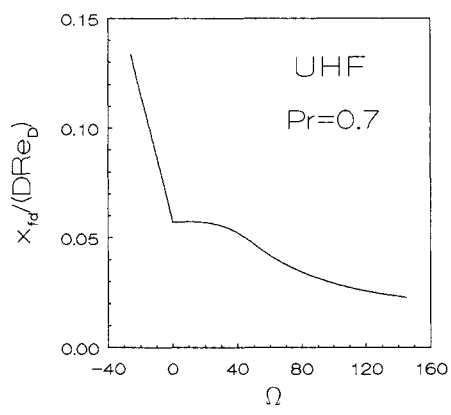

Fig. 10 Flow-thermal entry length in a uniformly heated or cooled vertical tube, $Pr = 0.7$.

As the buoyancy force is increased for a uniformly heated/cooled vertical tube, flow reversal results for both buoyancy

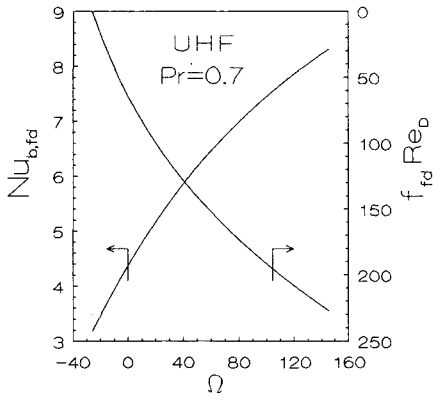

Fig. 11 Fully developed friction factors and bulk Nusselt numbers in a uniformly heated or cooled vertical tube, $Pr = 0.7$.

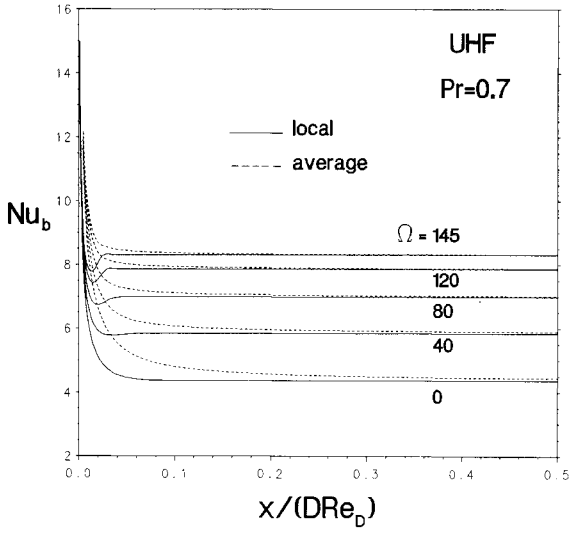

Fig. 12 Bulk Nusselt numbers for buoyancy assisting flow in a uniformly heated or cooled vertical tube, $Pr = 0.7$.

assisting and buoyancy opposing situations. Even though for the uniform heat flux case the buoyancy force is always present, if the flow becomes fully developed before flow reversal occurs, no reversal can occur further downstream. When the buoyancy assists the flow, the flow reversal is first detected at the centerline of the pipe at an axial location moderately farther from the inlet, $[x/(DRe_D)]_{crit} = 0.025$, than that for the uniform wall temperature case. On the other hand, when the buoyancy opposes the flow, the onset of the flow reversal which occurs in the immediate vicinity of the pipe wall, is shifted significantly downstream from the inlet at $[x/(DRe_D)]_{crit} = 0.101$. Flow reversal for the UHF case, as evidenced from Fig. 10, is found to occur very near the location where the flow and heat transfer approach fully developed conditions. For the uniformly heated/cooled vertical tube, the critical buoyancy parameters for which flow reversal is first detected were determined as $\Omega_{crit} = 146$ for buoyancy assisting and $\Omega_{crit} = -27$ for buoyancy opposing flow, respectively. As the magnitude of the buoyancy force is increased further, the initial flow reversal occurs upstream towards the inlet. Scheely and Hanratty[21] report flow reversal from an approximate fully developed flow analysis at $\Omega_{crit} = 159.6$ and $\Omega_{crit} = -26.1$, respectively, for assisting and opposing flow cases. Transition data for both upflow and downflow of water in a uniformly heated tube section are also reported[21] in terms of Gr/Re plots.

Consistent with the trends discussed friction factors, bulk Nusselt numbers are found to behave in a similar but less severe fashion (Figs. 12 and 13). Thus, for the buoyancy assisting case, local Nusselt numbers also exhibit slight valleys for all $\Omega > 0$ values plotted, and even less severe peaks at

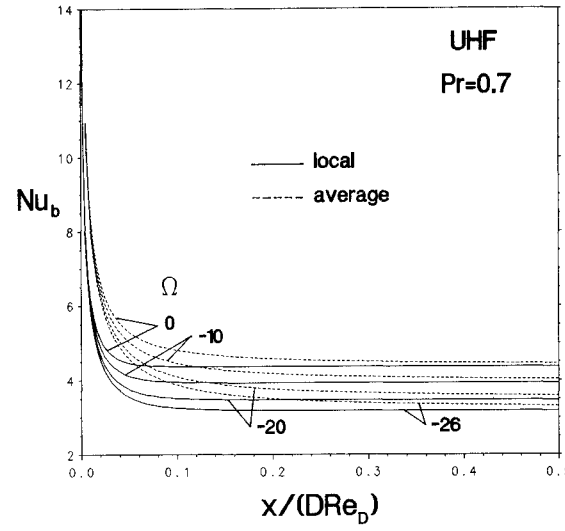

Fig. 13 Bulk Nusselt numbers for buoyancy opposing flow in a uniformly heated or cooled vertical tube, $Pr = 0.7$.

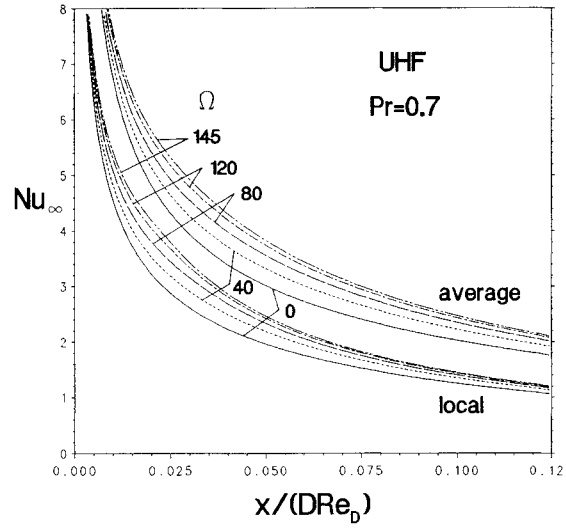

Fig. 14 Ambient Nusselt numbers for buoyancy assisting flow in a uniformly heated or cooled vertical tube, $Pr = 0.7$.

high buoyancy parameters $\Omega > 80$ as shown in Fig. 12. For the buoyancy opposing case ($\Omega < 0$), the bulk Nusselt numbers which lie below their corresponding zero buoyancy values decrease monotonically to their fully developed values as shown in Fig. 13. Fully developed bulk Nusselt numbers for both buoyancy assisting and opposing flow situations are also shown in Fig. 11.

Local and average ambient Nusselt numbers that inversely signify the dimensionless magnitude of tube wall temperature are plotted in Figs. 14 and 15 for buoyancy assisting and opposing flows, respectively. In contrast to the uniform wall temperature heating or cooling data shown in Figs. 6 and 7, the local ambient Nusselt numbers for the uniform heat flux case always exceed corresponding local forced convection data when buoyancy assists the flow (Fig. 14), whereas those for buoyancy opposing flow are always lower than forced convection data (Fig. 15). This is due to the continuous presence of the buoyancy forces. As the ambient Nusselt numbers are inversely proportional to the pipe wall temperature, the merging of the lines in Figs. 14 and 15 at large axial distances is not an indication of the disappearance of the buoyancy force, but instead is due to the increase of the denominator of the Nusselt numbers [Eqs. (10) and (12)]. The wall temperatures are therefore distinctly different for the various buoyancy parameters for all $x/(DRe_D)$ values. Again, with the aid of Eqs. (10) and (12), once the local and average wall temper-

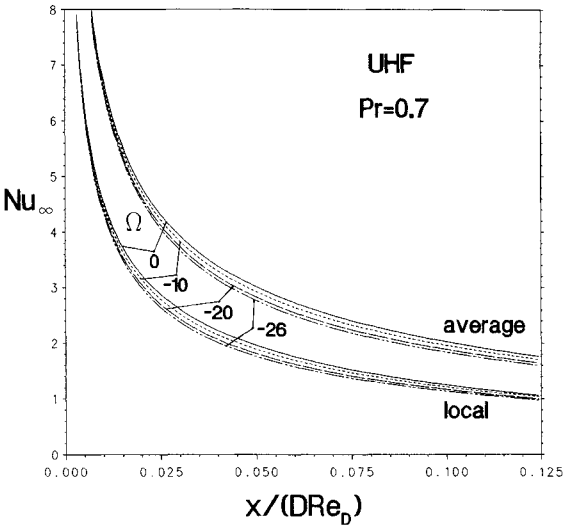

Fig. 15 Ambient Nusselt numbers for buoyancy opposing flow in a uniformly heated or cooled vertical tube, $Pr = 0.7$.

atures are calculated from Figs. 14 and 15, local and mean bulk temperatures can be determined from Figs. 12 and 13.

Conclusions

A numerical investigation is carried out to document the buoyancy effects in an isothermally or uniformly heated/cooled vertical tube for steady laminar mixed convection flow of air ($Pr = 0.7$). When the pipe is heated or cooled isothermally, the buoyancy force diminishes downstream as the fluid-to-wall temperature differences dwindle. Mixed convection velocity profiles attain the forced convection fully developed parabolic shape at significantly longer flow and thermal entry lengths for both buoyancy assisting and opposing flows. As the buoyancy force is the largest at the flow entrance, flow reversal for an isothermally heated or cooled vertical tube occurs very close to the entrance; at the center of tube for buoyancy assisting, and near the wall for the buoyancy opposing case.

When the vertical pipe is heated or cooled at a uniform rate, the buoyancy force persists throughout the heating/cooling region. Consequently, a single developing region for both velocity and temperature prevails. For buoyancy assisting flows, fully developed conditions are attained sooner than forced convection case as the velocity profiles exhibit maxima near the wall. For the buoyancy opposing flow, on the other hand, fully developed conditions are delayed with centerline velocities exceeding corresponding pure forced convection data. The onset of flow reversal for a uniformly heated/cooled tube shifts downstream away from the entrance, particularly for the buoyancy opposing case.

The opposing effects of the frictional forces and the buoyancy forces when $\Omega > 0$, results in local friction factors and local bulk Nusselt numbers that exceed their corresponding zero buoyancy values while exhibiting valleys and peaks particularly at high buoyancy intensities. On the other hand, when $\Omega < 0$, the buoyancy forces act in the same direction with frictional forces in slowing down the near-the-wall fluid, resulting in friction factors and bulk Nusselt numbers that lie below their corresponding zero buoyancy values. They either monotonically decrease to their fully developed values (UHF), or exhibit valleys in attaining their zero buoyancy fully developed limits (UWT).

References

[1]Martinelli, R. C., and Boelter, L. M. K., "The Analytical Prediction of Superposed Free and Forced Viscous Convection in a Vertical Pipe," *University of California Publications in Engineering*, Vol. 5, No. 2, 1942, pp. 23–58.

[2]Kays, W. M., "Numerical Solutions for Laminar-Flow Heat Transfer in Circular Tubes," *Transactions of the ASME*, Vol. 77, Nov. 1955, pp. 1265–1274.

[3]Hallman, T. M., "Combined Forced and Free-Laminar Heat Transfer in Vertical Tubes with Uniform Internal Heat Generation," *Transactions of the ASME*, Vol. 78, Nov. 1956, pp. 1831–1841.

[4]Siegel, R., Sparrow, E. M., and Hallman, T. M., "Steady Laminar Heat Transfer in a Circular Tube with Prescribed Wall Heat Flux," *Applied Scientific Research*, Sec. A, Vol. 7, No. 5, 1958, pp. 386–392.

[5]Hanratty, T. J., Rosen, E. M., and Kabel, R. L., "Effect of Heat Transfer on Flow Field at Low Reynolds Numbers in Vertical Tubes," *Industrial and Engineering Chemistry*, Vol. 50, No. 5, 1958, pp. 815–820.

[6]Jackson, T. W., Harrison, W. B., and Boteler, W. C., "Combined Free and Forced Convection in a Constant-Temperature Vertical Tube," *Transactions of the ASME*, Vol. 80, April 1958, pp. 739–745.

[7]Scheely, G. F., Rosen, E. M., and Hanratty, T. J., "Effect of Natural Convection on Transition to Turbulence in Vertical Pipes," *Canadian Journal of Chemical Engineers*, Vol. 38, June 1960, pp. 67–73.

[8]Morton, B. R., "Laminar Convection in Uniformly Heated Vertical Pipes," *Journal of Fluid Mechanics*, Vol. 8, June 1960, pp. 227–240.

[9]Kemeny, G. A., and Somers, E. V., "Combined Free and Forced-Convective Flow in Vertical Circular Tubes-Experiments with Water and Oil," *Journal of Heat Transfer*, Vol. 84, Nov. 1962, pp. 339–346.

[10]Ulrichson, D. L., and Schmitz, R. A., "Laminar-Flow Heat Transfer in the Entrance Region of Circular Tubes," *International Journal of Heat and Mass Transfer*, Vol. 8, Feb. 1965, pp. 253–258.

[11]Worsøe-Schmidt, P. M., and Leppert, G., "Heat Transfer and Friction for Laminar Flow of Gas in a Circular Tube at High Heating Rate," *International Journal of Heat and Mass Transfer*, Vol. 8, Oct. 1965, pp. 1281–1301.

[12]Lawrence, W. T., and Chato, J. C., "Heat-Transfer Effects on the Developing Laminar Flow Inside Vertical Tubes," *Journal of Heat Transfer*, Vol. 88, May 1966, pp. 214–222.

[13]Marner, W. J., and McMillan, H. K., "Combined Free and Forced Laminar Convection in a Vertical Tube with Constant Wall Temperature," *Journal of Heat Transfer*, Vol. 92, Aug. 1970, pp. 559–562.

[14]Zeldin, B., and Schmidt, F. W., "Developing Flow with Combined Forced-Free Convection in an Isothermal Vertical Tube," *Journal of Heat Transfer*, Vol. 94, May 1972, pp. 211–223.

[15]Mullin, T. E., and Gerhard, E. R., "Heat Transfer to Water in Downward Flow in a Uniform Wall Temperature Vertical Tube at Low Graetz Numbers," *Journal of Heat Transfer*, Vol. 99, Nov. 1977, pp. 586–589.

[16]Greif, R., "An Experimental and Theoretical Study of Heat Transfer in Vertical Tube Flows," *Journal of Heat Transfer*, Vol. 100, Feb. 1978, pp. 86–91.

[17]Collins, M. W., "Heat Transfer by Laminar Combined Convection in a Vertical Tube-Predictions for Water," *Proceedings of the Sixth International Heat Transfer Conference*, Toronto, Canada, 1978, pp. 25–30.

[18]Kasz, J., and Dylag, M., "Combined Free and Forced Convection in the Entrance Region of a Vertical Tube," 9th CHISA Congress, Prague, Czechoslovakia, 1987.

[19]Collins, M. W., "Finite Difference Analysis for Developing Laminar Flow in Circular Tubes Applied to Forced and Combined Convection," *International Journal for Numerical Methods in Engineering*, Vol. 15, 1980, pp. 381–404.

[20]Gebhart, B., Jaluria, Y., Mahajan, R. L., and Sammakia, B., *Buoyancy-Induced Flows and Transport*, Hemisphere, Washington, DC, 1988.

[21]Scheely, G. F., and Hanratty, T. J., "Effect of Natural Convection on Stability of Flow in a Vertical Pipe," *Journal of Fluid Mechanics*, Vol. 14, Oct. 1962, pp. 244–258.

[22]Scheely, G. F., and Hanratty, T. J., "Effect of Natural Convection Instabilities on Rates of Heat Transfer at Low Reynolds Numbers," *AIChE Journal*, Vol. 9, No. 2, 1963, pp. 183–185.

[23]Patankar, S. V., *Numerical Heat Transfer and Fluid Flow*, Hemisphere, Washington, DC, 1980.

[24]Patankar, S. V., and Spalding, D. B., "A Calculation Procedure for Heat, Mass, and Momentum Transfer in Three-Dimensional Parabolic Flow," *International Journal of Heat and Mass Transfer*, Vol. 15, Oct. 1972, pp. 1787–1806.

[25]Rosen, E. M., and Hanratty, T. J., "Use of Boundary-Layer Theory to Predict the Effect of Heat Transfer on the Laminar-Flow Field in a Vertical Tube with a Constant-Temperature Wall," *AIChE Journal*, Vol. 7, No. 1, 1961, pp. 112–123.